7 Particle Physics at DESY/HERA (H1)

J. Becker, Ilaria Foresti, S. Hengstmann, M. Hildebrandt, N. Keller, J. Kroseberg, Katharina Müller, P. Robmann, F. Sefkow, U. Straumann, P. Truöl, M. Urban, R. Wallny and Nicole Werner

in collaboration with:
R. Eichler, W. Erdmann, C. Grab, M. Hilgers, H.-C. Kästli (until May 2000), B. List, S. Lüders, D. Meer and A. Schöning, Institut für Teilchenphysik der ETH, Zürich,
S. Egli, K. Gabathuler, J. Gassner, and R. Horisberger, Paul–Scherrer–Institut, Villigen, and 34 institutes outside Switzerland

(**H1**–Collaboration)

7.1 Electron-proton collisions at up to 320 GeV center of mass energy: overall status of the project

In its last year before the major upgrade the HERA electron/positron-proton storage ring operated with positrons. A total luminosity of 56 pb^{-1} was accumulated. The big shutdown originally planned for May 2000 was delayed until September to let the HERA-B experiment take first physics data, and also to adapt for delivery delays of various components needed for the upgrade of HERA, the H1- and the ZEUS-experiment. The luminosity in the year 2000 constitutes 40 % of what is available for e^+p collisions altogether (see Table 7.1).

Table 7.1: *Summary of HERA and H1 operation during the previous nine years.*

		e^-p	e^+p		
Parameter		1992-94, 1998/99	1994-99	2000	Sum
Integrated luminosity $\mathcal{L}$					
HERA produced	$[\mathrm{pb}^{-1}]$	28.3	95.8	69.5	165.3
HERA physics	$[\mathrm{pb}^{-1}]$	26.6	90.0	66.8	156.8
H1 taken	$[\mathrm{pb}^{-1}]$	22.7	71.6	59.4	131.0
H1 physics	$[\mathrm{pb}^{-1}]$	19.9	65.1	56.2	121.3
HERA efficiency	[%]	94	94	96	95
H1 efficiency	[%]	75	72	84	77
Average luminosity	$[(\mu\mathrm{b\ s})^{-1}]$	3.15	3.64	6.47	4.83
Peak luminosity	$[(\mu\mathrm{b\ s})^{-1}]$	12.1	12.6	17.9	17.9
Average p current	[mA]	67.5	70.6	86.7	77.4
Average $e^\pm$ current	[mA]	17.2	22.9	25.1	23.8
HERA luminosity runs		700	1376	346	1722
Permanent H1 runs	$[10^3]$	9.6	18.7	6.0	24.7
Average duration	[min]	20	22	28	25

Most of our publications use pre-1998 data only. A major effort, part of which is described below, was undertaken to improve the calibration and alignment of tracker components. After this was accomplished the reprocessing of the 1999/2000 data has recently been started. In 15 publications [1]-[15] of the collaboration the following principal areas are covered:

- neutral and charged electroweak current cross sections, proton structure functions and parton densities at high momentum transfer Q^2 [2, 13, 14],

- search for states outside the standard model [4, 9, 15],
- photon structure [5],
- parton-fragmentation into multijet final states [1, 10, 11, 12],
- electroproduction of exclusive final states [7, 8], and
- production of heavy quark-antiquark states, of open charm and beauty [6].

We will report below on the analyses in the heavy quark sector (Sect. 7.4.1), an area where there is manifest activity of the University of Zürich group, and also give an update of the high Q^2 data. The latter results are based also on data taken in 2000, have not been published, but were included in the 36 contributions of our collaboration to the ICHEP-2000 conference [16].

With the submission of a publication [13] and the thesis the analysis project of Rainer Wallny has been concluded. This work deals with deep-inelastic inclusive ep scattering at low x and a measurement of α_s, and was discussed in detail in our previous annual report Another Zürich analysis project (thesis of Nikolas Keller) concerns QED Compton scattering. Events with both the scattered electron and the radiated photon within the main detector are investigated and will ultimately allow a comparison of the photon and gluon distributions within the proton.

Besides the physics analysis, our activities dealt with the maintenance, monitoring and calibration of the detector components built in Zürich for the central tracker and the first level trigger of H1. Most of our effort, however, was directed towards the H1 detector upgrade which progressed with minor delays. At present the H1-detector is ready for the installation of the first superconducting focussing magnet into the forward tracker. The central tracker, with the exception of the silicon detectors, is installed too. One element, the superconducting coil used to compensate the influence of the H1-analysing magnetic field on the proton beam, has now become obsolete. This element, indispensable for high luminosity tuning, was manufactured by Swiss industry and largely financed by University of Zürich funds. It functioned without problems for ten years. Figure 7.1 show the magnet on its way to storage.

Figure 7.1: *Left: The superconducting compensator coil is being taken out of the beam line (October 2000). Right: Installation of the new central inner proportional chamber (CIP) into the central tracking device of the H1 Detector in Hamburg. The central jet chambers (CJC) which surround the CIP can be seen, too (February 2001).*

7.2 Summary of activities related to the H1-upgrade

As part of the H1 upgrade the two inner proportional chambers (CIP) and the inner drift chamber (CIZ) are replaced by a new five-layer proportional chamber (CIP2000). The aim is to improve z-vertex triggering and track reconstruction at the trigger level, as well as background rejection. The number of readout channels both in z and in azimuthal direction have increased. Five layers rather than two will provide redundancy and help resolve ambiguities in the track reconstruction of the central silicon tracker. The new CIP has pad readout in 16 azimuthal sectors. The trigger scheme is based on a projective pad geometry in the z direction, thus resulting in a varying number of pads per layer (ranging from 119 to 93 for the innermost and outermost layer, respectively). The larger number of detector channels also required new readout and trigger electronics.

The project was coordinated by the Unversity of Zürich with ETH Zürich and University of Heidelberg as partners. The University of Zürich was responsible for the design and construction of the multiwire proportional chambers. The construction started in autumn 1999 and was completed by the end of 2000.

The ASIC laboratory in Heidelberg developed the amplifier and readout chip CIPix, and the electronics for trigger and data acquisition is a common Heidelberg and Zürich University effort. ETH Zürich is responsible for all components dealing with the optical data transmission from the detector to the electronic trailer.

Meanwhile the new chamber has been installed in the H1 detector. Further details are given below.

7.2.1 Central inner proportional chamber construction

Between July 1999 and February 2001 three to five people worked permanently on the construction and test of the new chamber which consists of an innermost layer with anodes only, four layers with cathode pads inside and anode wires outside and an outermost layer with only readout pads, all planes including readout cabling. 2400 anode wires were strung at the Paul-Scherrer-Institut Villigen (PSI) on provisional frames and soldered to the detector in Zürich. To guarantee a stable wire position the tension has to be around 80 g. Every individual wire has been tested, 30 of which had to be exchanged.

After the assembly of the whole chamber in December 2000 the first high voltage test took place. Due to two broken wires the chamber had to be reopened for a short time. From December to January the high voltage was increased up to the operation point of 2395 V and first signals were seen. Until February last wire problems had been solved, thus all layers operate at 2500 V. Fitting the cooling units to the readout electronic boards turned out to be a difficult task, but a solution was found. The chamber survived the transport from Zürich to Hamburg without any harm. Due to a glue seam at the $+z$ end of the Central Jet Chamber the CIP is now installed 1 mm shifted in backward direction. The readout prints are planned to be mounted at the beginning of April 2001.

7.2.2 CIP Electronics

Last year several tests of the readout electronics from PSI have been performed with the CIP prototype including the CIPix card and receiver card prototypes. Amongst others the pulse shape, efficiency and time resolution have been studied [17].

In order to measure the time resolution a ^{106}Ru β source was placed upon the CIP prototype and two scintillators on top and on bottom of the chamber acted as a coincidence

indicator for particles passing through. The HERA bunch structure was simulated by selecting tracks within 24 ns of the rising edge of a 10 MHz clock. The delay Δt of the signal readout was shifted between 0 and 70 ns and the number of signals coming from the correct bunch crossing devided by all coincidence signals was measured. This fraction is required to become one within significantly less than one bunch crossing. The resolution is measured to be better than 50 ns as can be seen in Fig. 7.2.

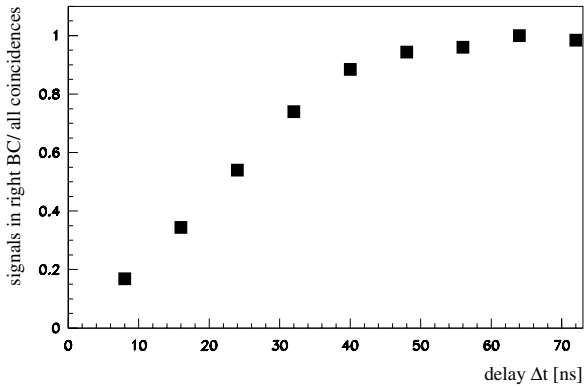

Figure 7.2: *Efficiency of the CIP prototype v.s. gate delay measured with a ruthenium source.*

In February 2001 part of the readout electronics was connected to the chamber and tested for the first time. Eight CIPix chips on the fifth chamber layer were connected to receiver cards through two optical links. The programming of the CIPix chips via an I^2C-Bus has been developed in the framework of a diploma thesis [17]. After the usual grounding problems had been solved, pulse shapes as shown in Fig. 7.3 were recorded. The pulses were measured by using a scintillator coincidence as a trigger for tracks induced by the source. In addition to the analog pulse the digital signal is displayed in Fig. 7.3.

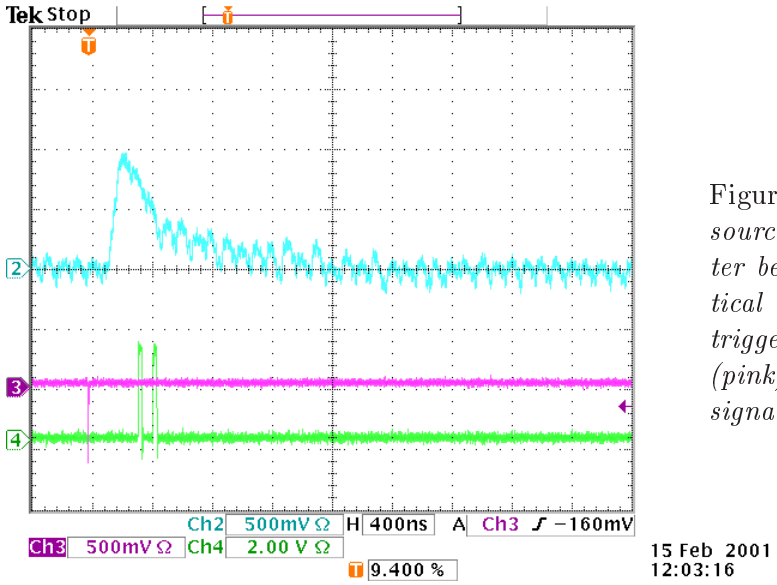

Figure 7.3: *Signals from a ruthenium source from layer 5 of CIP2000, after being transmitted through the optical link. The analog pulse (blue) triggered by a scintillator coincidence (pink) is transformed into a digital signal (green) on the CIPix chip.*

The same setup was used to measure the first efficiency curve of the CIP2000. The plateau starts at around 2300 V which is comparable to the value of the old CIP. For the inner layers, which have narrower interwire spacing, the required voltage will be slightly higher.

The assembly of all CIPix and receiver cards with optical hybrids for all layers is now going on at PSI and expected to be finished at the end of March 2001. The mounting of the frontend electronics to the chamber is planned for April.

The trigger electronics has been developed and built together with the electronics workshop of the University of Heidelberg [18]. All trigger cards have been successfully tested and are ready since February 2001. In order to build trigger elements for the H1 trigger system, signals from the CIP2000 are readout in form of trigger histograms. These histograms are calculated by sum cards which are under construction and are expected to be ready in April.

For details about the data acquisition and control system of the CIP2000 see [19].

7.3 A new era of tracking at H1

The capability to detect heavy quarks through their lifetime broadens the scope of the HERA physics programme considerably. New possibilities arise not only for testing QCD and probing aspects of hadronic structure, but also for searches for processes beyond the Standard Model in which long-lived particles are produced. To resolve the secondary vertices of e.g. b hadrons with a mean life corresponding to $c\tau = 470\,\mu$m requires an excellent tracking performance; the efficiency to tag b hadrons and suppress background is directly related to the precision with which tracks from the secondary decay vertices can be reconstructed.

To fully exploit the potential of the H1 silicon micro-vertex detector (CST), it is therefore necessary to optimize the performance of the entire tracking system. To achieve this goal, the H1-collaboration has launched a dedicated tracking task force in autumn 1999 convened by F. Sefkow. The main project is a complete and consistent recalibration and alignment of the entire tracking system. The studies are based upon 10^7 cosmic muon triggers, which were recorded especially for this purpose. The alignment benefits from the enhanced redundancy and precision induced by the CST information into the tracking system, shown in Fig. 7.4.

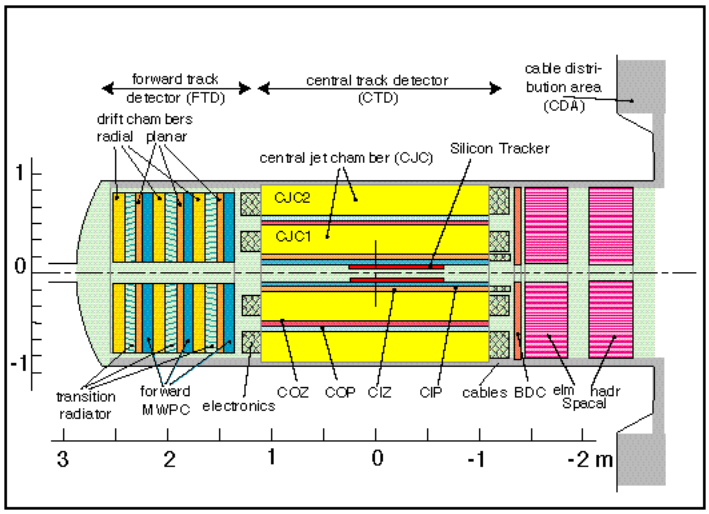

Figure 7.4: *Schematic side view of the tracking system.*

A frequent problem in tracking alignment is that reference tracks from one initially miscalibrated detector or detector part induce biases into the calibration of another, which requires lengthy iteration procedures. Such biases are avoided in the approach implemented in the MILLEPEDE program [20]. In this ansatz alignment and calibration parameters are called *global*, while individual track parameters are called *local*. Using the track information from many thousands of events the new fit algorithm allows for a simultaneous fit of all global and local parameters as an exact solution of a least squares minimisation problem. With $n = 10^3$ global parameters, typically, and $N = 10^4 \ldots 10^6$ track parameters, this corresponds to the inversion of a huge $(N + n) \times (N + n)$ matrix, a problem which can be reduced to solvable size in MILLEPEDE because only the global parameters need to be explicitly known.

Focusing on the central z-chamber (CIZ), built at our institute, we briefly outline the new fit technique and present the improvements (Thesis S. Hengstmann). The CIZ is a drift chamber subdivided into 15 rings in z with in total 60 sense wires strung concentrically and perpendicular around the beam axis, to measure the z coordinate of tracks. The local track-model of the z-chamber is given by the equation $z = z_0 + \lambda \cdot S$, where S denotes the transverse arc-length of the track and z_0 and λ are the straight line fit parameters with $\lambda = cot(\theta)$. The geometrical alignment and calibration constants are global translations (Δx, Δy) and rotations (γ, ψ, ω) around the z, x and y-axis, wirewise z-shifts $\Delta z^1, \Delta z^2, ..., \Delta z^{60}$, drift velocities v_d and drift time corrections $t_0^1, t_0^2, ..., t_0^{60}$. They can be integrated into one global fit-vector

$$\vec{P} = (\Delta x, \Delta y, \gamma, \psi, \omega, v_d, t_0^1, t_0^2, ..., t_0^{60}, \Delta z^1, \Delta z^2, ..., \Delta z^{60}) \tag{7.1}$$

and the local track model can be expanded to the form

$$z_{Hit} = z_0 + \lambda \cdot S_{Hit} + \vec{A} \cdot \vec{P} \ , \tag{7.2}$$

where the vector $\vec{A}$ contains the derivatives $\partial z / \partial \vec{P}$, which have to be supplied in analytic form to MILLEPEDE. Similar formulae are valid for the outer z-chamber (COZ) which has 96 wires. The new z-coordinate fit determines the more than 300 CIZ and COZ alignment and calibration constants in a single step. It uses a large sample of cosmics precisely measured by the CST, together with tracks outside the CST acceptance. The simultaneous fit ensures that the precise constraints of the CST are propagated to the entire z-chamber system.

Results of the re-calibration are presented in Fig. 7.5. Here only central rings are shown, which almost fully overlap with the CST. In a first step correction the hit resolution has already been improved from 800 μm to 500 μm. With the final step, displayed here, remaining shifts in the residual distribution of δz indicating a misalignment vanish and the resolution improves further almost uniformly to $\sigma_z = (378 \pm 5)$ μm. This result is consistent with the intrinsic resolution, as determined from hit triplets.

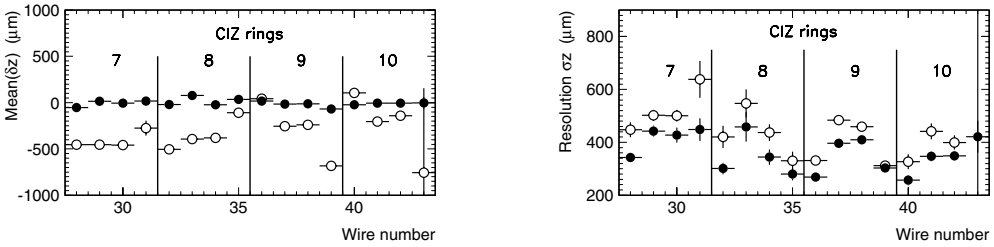

Figure 7.5: *(a) Residuals δz and (b) resolution σ_z versus wire number before (open dots) and after (full dots) the new z calibration.*

A complete re-calibration of the central jet chamber (CJC) has also been performed in the framework of the new fit using the precise CST information as a constraint. With the two cylindrical, coaxial drift volumes (CJC1 and CJC2) (see Fig. 7.4) consisting of in total 90 cells and 56 wire planes parallel to the beam axis, about 1000 parameters have to be fitted to calibrate the track measurement in the $r\phi$-plane. Special corrections accounting for inhomogeneities of the drift region and the magnetic field, pulse shape dependence, time-of-flight, etc., have also been applied. An improvement of the resolution by about 40 % for the track parameters distance of closest approach d_{ca}, ϕ and $1/p_t$ is observed consistent with a

gain in the single hit resolution from 240 μm to 140 μm in the $r\phi$-plane, which is the design value.

The new algorithm has also been applied to calibrate the CJC z-position and energy-loss (dE/dx) measurement, determined from the charge amplitudes on opposite ends of the wires. The amplitudes are highly correlated and show moderate resolutions. Furthermore they depend on the gas pressure, the electron current in HERA, on the track angle θ and there are effective corrections to the Bethe-Bloch formula. Considering all effects almost 8000 calibration constants have to be fitted. For this procedure a consistent calibration of the z-chambers (CIZ and COZ) was found to be essential.

The complete alignment and calibration of the CST requires the determination of 384 parameters. The combined CST+CJC track fit yields an impact parameter resolution of about 30 μm which is again according to design and similar to values achieved in LEP detectors.

The total integrated luminosity that benefits from the recalibration amounts to about 100 pb^{-1}. The data have been taken during the years 1997 to 2000 and are currently reprocessed at H1. To account for time-dependent beam line parameters and calibration constants, e.g. drift velocities, two reconstruction passes are needed. An online version of the new fit algorithm has been implemented into the reconstruction software to determine these parameters in the first pass. Afterwards the results are fed into a second pass of the final re-processing. For this dual procedure a time-frame of 4 - 5 month is estimated. It is currently on track to finish before the end of the present shutdown.

7.4 Results from recent analyses

7.4.1 Beauty production

The important contributions of our group to track-based triggering and to precision tracking continue to be complemented by a strong analysis effort in the field of heavy quark production, which critically relies on these detector capabilities.

The heavy quarks, by virtue of their mass, provide an ideal test bed to explore the range of applicability of perturbative QCD. Furthermore, since in the QCD picture of ep interactions, heavy quarks are predominantly produced in the interaction of a real or virtual photon emitted from the scattered electron with a gluon in the proton, they carry direct messages about the gluons entering the hard scattering process.

Most results so far were obtained with charm quarks. We have used the clean experimental signature of D^* mesons [21] to measure the gluon density in the proton, and to probe the rôle of gluons in the dynamics of diffractive interactions [22] (Thesis S. Hengstmann). In comparison, relatively little is known so far about the production of beauty quarks at HERA, which is about 100 times less abundant than charm. Only the magnitude of the photo-production cross section has been measured [23] so far and found larger than expected. In DIS, beauty production has not yet been observed at all.

Whereas the theoretical description of charm production is found to be in reasonable agreement with data, not only at HERA, it appears to be difficult to reproduce the high beauty production rates with QCD calculations, even when next-to-leading order terms are included. The problem is known for some time for $\bar{p}p$ collisions [24], but similar discrepancies are seen in photo-production and have recently also been reported from high energy two-photon collisions at LEP [25]. These observations are in remarkable contrast to the expectation that contributions from higher orders should be smaller in the case of beauty than for charm, due to the larger mass scale, so that the theory should be more reliable, and they have thus given rise to speculations about contributions from non-standard production mechanisms (e.g. [26]).

Measurements at HERA can provide important clues to better understand beauty production, since, compared to $\bar{p}p$, γp and $\gamma\gamma$ interactions uncertainties due to imprecise knowledge of hadronic structure are smallest in ep scattering.

In this field, we could in the last year harvest the first fruits from our efforts to integrate the central silicon tracker [27] (CST) into the analysis. We confirmed the earlier photo-production measurement by using an independent, lifetime-based signature [28], and we succeeded in performing a first measurement of beauty production in DIS [29] (Thesis J. Kroseberg).

All H1 measurements are done using event samples with two jets accompanied by a muon identified as penetrating track in the instrumented iron and well measured in the CST. They rely on the signature of semileptonic decays of b hadrons in jets. The previous H1 measurement was based on the high transverse momentum p_T^{rel} with respect to the jet direction, which the lepton acquires due to the higher b mass. The long lifetimes of b hadrons, which can be measured with micro-vertex detectors, provide an independent signature. For each muon candidate, the impact parameter δ is calculated in the plane transverse to the beam axis. Its magnitude is given by the distance of closest approach of the track to the primary event vertex. Its sign is positive if the intercept of the track with the jet axis is downstream of the primary vertex, and negative otherwise. Decays of long-lived particles are signalled by positive impact parameters, whereas the finite track resolution yields a symmetric distribution.

The b cross section is extracted by decomposing the impact parameter distribution, Fig. 7.6. The fit yields a beauty fraction of $f_b = (26 \pm 5)\%$ which translates into a cross

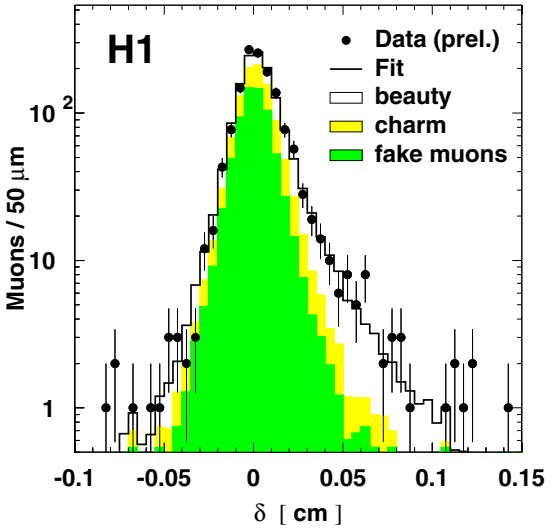

Figure 7.6: *Impact parameter distribution and decomposition from the likelihood fit.*

section consistent with the published result, based on earlier data, within the statistical error.

One can enrich the b component in the events by restricting the range of one variable, e.g. p_T^{rel} and then studying the distribution of the other quantity, δ, and *vice versa*. Fig. 7.7 shows a clean beauty signature in both observables.

The two variables δ and p_T^{rel} complement each other in the discrimination of the beauty component in the data against the different background sources. The separation power can be combined in a likelihood fit of the two-dimensional distribution of these quantities. The result, averaged with the published number, is $\sigma(ep \to b\bar{b}X \to \mu X) = (170 \pm 25)\,\mathrm{pb}$ in the range $Q^2 < 1$ GeV^2, $0.1 < y < 0.8$, $p_T(\mu) > 2$GeV, $35^\circ < \theta(\mu) < 130^\circ$. This is significantly higher than the NLO QCD prediction.

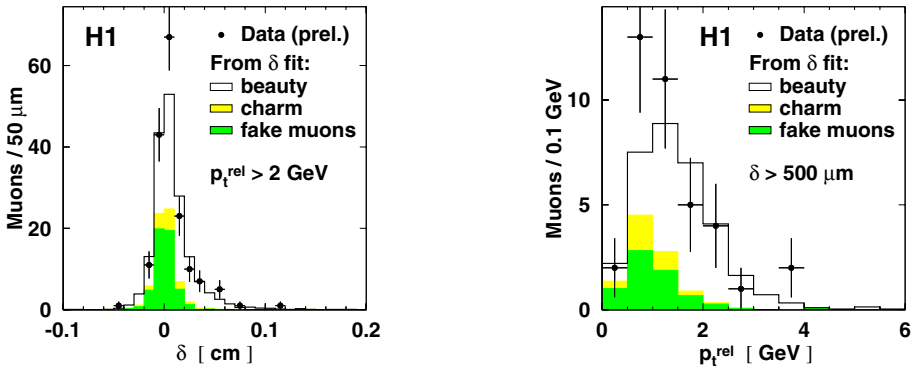

Figure 7.7: *Impact parameter distribution for muon candidates with $p_T^{rel} > 2$ GeV (a) and p_T^{rel} distribution for muon candidates with $\delta > 500$ μm (b), with estimated contributions.*

The same method has been applied to obtain the first measurement of b production in DIS, where the statistics is considerably lower. The likelihood fit of the reference spectra to the two-dimensional distribution in δ and p_T^{rel} yields a $b\bar{b}$ fraction of $f_b = (43 \pm 8)\,\%$. The projections of this distribution are shown in Fig. 7.8 together with the decomposition from the fit. The distributions of both variables are well described, and the need for a $b\bar{b}$ component is evident from the lifetime based signature as well as from the p_T^{rel} spectrum. The cross section in the visible range $2 < Q^2 < 100$ GeV^2, $0.05 < y < 0.7$, $p_T(\mu) > 2$ GeV

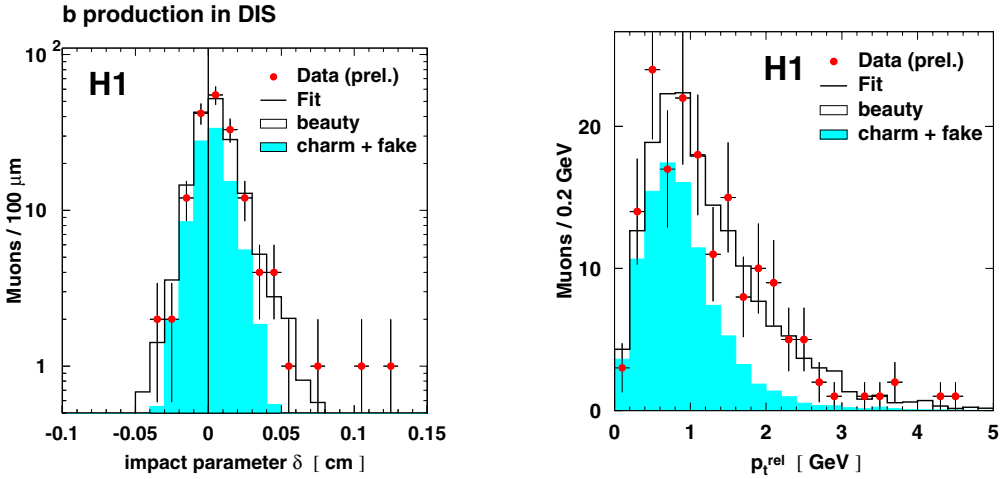

Figure 7.8: *Impact parameter distribution (left), and distribution of transverse momentum relative to the jet axis (right), with decomposition from the likelihood fit.*

and $35^\circ < \theta(\mu) < 130^\circ$ is found to be

$$\sigma_{vis}(ep \to b\bar{b}e'X \to \mu X) = 39 \pm 8\ (stat.) \pm 10\ (syst.)\ \text{pb}\ .$$

This measurement can be directly compared to a NLO QCD calculation, which gives (11 ± 2) pb. A similar excess as observed in $\bar{p}p$, γp and $\gamma\gamma$ interactions is now also seen in ep scattering.

In order to subject the theory to more refined tests, for example by measuring differential distributions, or to extend the probed phase space, more efficient ways of tagging beauty quarks are necessary, which becomes possible by making use of the CST information also in hadronic decay channels. This approach is followed in the thesis work of I. Foresti.

7.4.2 Update on high Q^2 data

The analyzed e^-p data taken in 1998 and 1999 at a center-of-mass energy of 320 GeV correspond to an integrated luminosity of 15.3 pb^{-1}. From these data inclusive single and double differential cross sections for neutral and charged current in the range of four-momentum transfer squared Q^2 between 200 and 30 000 GeV^2, and Bjorken x between 0.0032 and 0.65 are extracted [30]. When these data are compared with our measurements of the inclusive neutral and charged current e^+p cross sections clear evidence is observed for neutral current parity violating Z^0 exchange and the structure function F_3 can be extracted. The data are found to be in good agreement with Standard Model predictions (see Fig. 7.9).

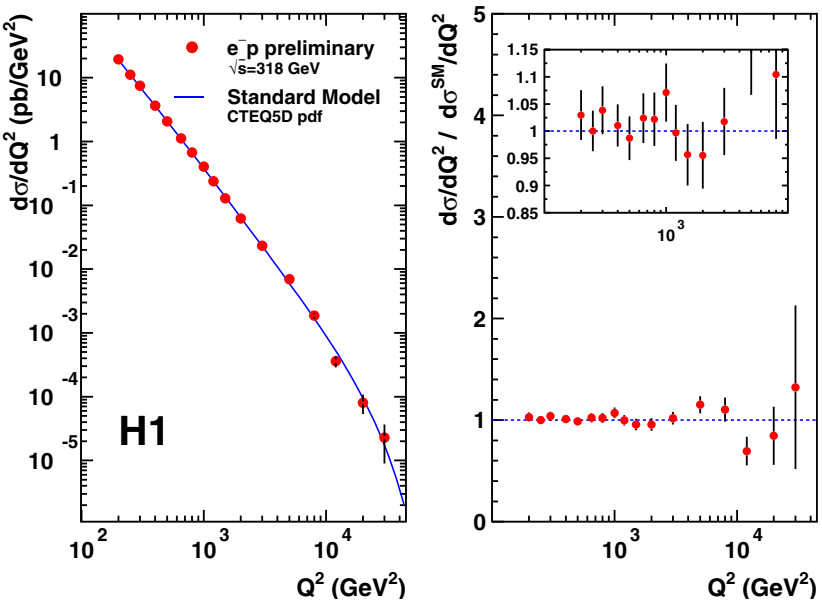

Figure 7.9: *Differential cross sections $d\sigma/dQ^2$ at 318 GeV centre-of-mass energy for $e^-p \to e^-X$. The H1-data are compared to Standard model expectations using the CTEQ5D [34] parton density functions. (Extracted from ref. [31])*

The same data are also used to search for eq contact interactions associated to scales not directly accessible at HERA [31]. For conventional contact interactions lower bounds can be set on eq compositeness scales $\Lambda^{\pm}$ at $1.6 - 9.2$ TeV and on leptoquarks with a ratio mass over coupling M/λ of $0.3 - 1.7$ TeV. A search for low scale gravitational effects through the exchange of Kaluza-Klein excitations of gravitons in models with large extra dimensions results in lower limits on the effective Planck scale M_S of 0.63 TeV and 0.93 TeV for positive and negative coupling, respectively.

The inclusive e^+p single and double differential cross sections measured in 1999 and 2000 in the same range of x and Q^2 were also analyzed. The data set corresponds to an integrated luminosity of 45.9 pb^{-1}. The cross-sections are compared to previous H1 results based on 35.6 pb^{-1} of data taken in 1994 to 1997 at $\sqrt{s} = 300$ GeV in Fig. 7.10. The new measurements are found to be fully consistent with previous ones and well described by next-to-leading order QCD fits in the framework of the Standard Model [32], as is apparent in Fig. 7.11.

The search for W boson production in the process $ep \to eWX$, with subsequent W decay into electrons or muons, has been continued using an integrated luminosity of 13.6 pb^{-1} in e^-p scattering and 81.6 pb^{-1} in e^+p scattering [33]. The analysis has been tuned to maximize the acceptance of W ($W \to e\nu$, $W \to \mu\nu$) boson production, and reject other

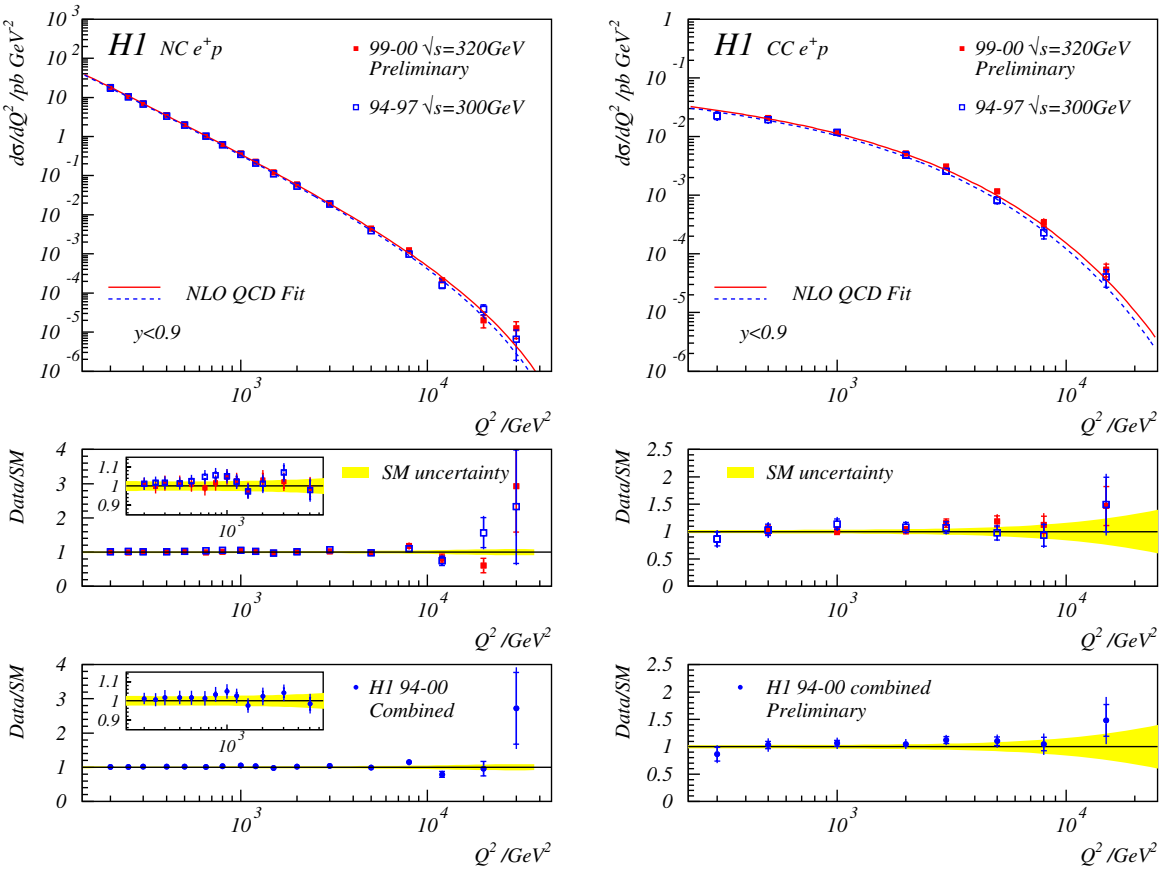

Figure 7.10: *The Q^2 dependence of the neutral current (NC,left) and charged current (CC,right) cross sections $d\sigma/dQ^2$ is shown for the new (1999/2000, solid points) and the old (1994/7, open points) measurements The lines indicate the results of a next-to-leading order QCD fit based on the pre-1997 H1 data, dashed at $\sqrt{s} = 300$ GeV and full for $\sqrt{s} = 320$ GeV. The ratio between data and Standard model fit is shown in figures (b) and (c). The latter includes both old and new data.*

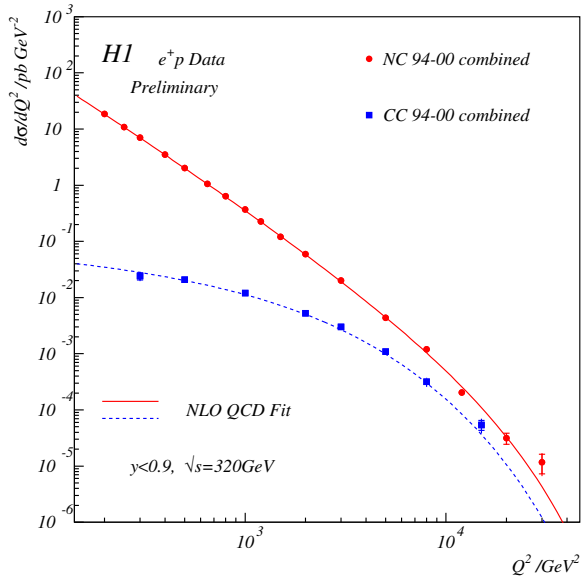

Figure 7.11: *The Q^2 dependence of the neutral current (NC) and charged current (CC) cross sections $d\sigma/dQ^2$ is shown for the combined 1994 - 2000 data. The lines indicate the results of a next-to-leading order QCD fit based on the pre-1997 H1 data.*

Standard Model processes like the charged and neutral current processes $ep \to \nu X; \to eX$, respectively or lepton pair production in $\gamma\gamma$ interactions. In e^-p interactions no events are observed, consistent with the expectation of the Standard Model in this low luminosity sample of 1.46 ± 0.30 (0.32 ± 0.09) for the e (μ) sample. In the e^+p data 14 events are seen, six in the electron and eight in the muon channel compared to an expectation of 6.14 ± 1.46 and 2.01 ± 0.54, respectively, or 8.2 ± 2.0 when taken together dominated by W production (6.4 ± 1.9). The excess above the expectation is mainly due to events with transverse momentum of the hadronic system greater than 25 GeV where 9 events are found compared to 2.3 ± 0.6 expected. Four of these events are observed in the latest data sample.

References

[1] *Measurement of Transverse Energy Flow in Deep-Inelastic Scattering at HERA*, H1-Coll., C. Adloff *et al.*, Eur. J. Phys. **C12** (2000), 595.

[2] *Measurement of Neutral and Charged Current Cross Sections in Positron-Proton Collisions at Large Momentum Transfer*, H1-Coll., C. Adloff *et al.*, Eur. J. Phys. **C13** (2000), 609.

[3] *Investigation of Power Corrections Event Shape Variables Measured in Deep-Inelastic Scattering*, H1-Coll., C. Adloff *et al.*, Eur. J. Phys. **C14** (2000), 255; addendum ibid. **C18** (2000), 417.

[4] *Search for Compositeness, Leptoquarks and Large Extra Dimensions in eq Contact Interactions at HERA*, H1-Coll., C. Adloff *et al.*, Phys. Lett. **B479** (2000), 358.

[5] *Measurement of Di-jet Cross Sections in Photoproduction and Photon Structure*, H1-Coll., C. Adloff *et al.*, Phys. Lett. **B483** (2000), 36.

[6] *Elastic Photoproduction of J/Ψ- and Y-Mesons at HERA*, H1-Coll., C. Adloff *et al.*, Phys. Lett. **B483** (2000), 23.

[7] *Elastic Φ-Meson Production at HERA*, H1-Coll., C. Adloff *et al.*, Phys. Lett. **B483** (2000), 360.

[8] *Inclusive Photoproduction of Neutral Pions in the Photon Hemisphere at HERA*, H1-Coll., C. Adloff *et al.*, Eur. J. Phys. **C18** (2000), 293.

[9] *A Search for Excited Fermions at HERA*, H1-Coll., C. Adloff *et al.*, Eur. J. Phys. **C17** (2000), 567.

[10] *Di-jet Production in Charged and Neutral Current ep Interactions at High Q^2*, H1-Coll., C. Adloff *et al.*, DESY 00 – 143, hep-ex 0010016, Eur. J. Phys. **C** (2001), in print.

[11] *Measurement and QCD Analysis of Jet Cross Sections in Deep-Inelastic Positron-Proton Collisions at $\sqrt{s}$ of 300 GeV*, H1-Coll., C. Adloff *et al.*, DESY 00 – 145, hep-ex 0010054, Eur. J. Phys. **C** (2001), in print.

[12] *Diffractive Jet-Production in Deep-Inelastic e^+p Collisions at HERA*, H1-Coll., C. Adloff *et al.*, DESY 00 – 174, hep-ex 0012051, Eur. J. Phys. **C** (2001), in print.

[13] *Deep-Inelastic Inclusive ep Scattering at Low x and a Measurement of α_s*, H1-Coll., C. Adloff *et al.*, DESY 00 – 181, hep-ex 0012053, subm. to Eur. J. Phys. **C**.

[14] *Measurements of Neutral and Charged Current Cross Sections in Electron-proton Collisions at High Q^2 at HERA*, H1-Coll., C. Adloff *et al.*, DESY 00 – 187, hep-ex 0012052, Eur. J. Phys. **C** (2001), in print.

[15] *Searches at HERA for Squarks in R-Parity Violating Supersymmetry*, H1-Collaboration, C. Adloff *et al.*, DESY 01 – 021, hep-ex 0102050. subm. to Eur. J. Phys. **C** (2001).

[16] H1-contributions to Int. Cong. on High-Energy Physics (ICHEP 2000), Osaka, Japan; available at *http://www-h1.desy.de/h1/www/publications/conf/list.ICHEP2000.html*

[17] A. Vollhardt, *Entwurf und Bau einer Frontend-Steuerung für das CIP-Upgrade Projekt für H1 bei HERA*, Diploma Thesis, January 2001.

[18] M. Urban, *Ein schneller Trigger für H1 bei HERA*, Diploma Thesis, May 2000.

[19] J. Becker, *The Data Acquisition and Control System for a Fast Trigger at H1*, Diploma Thesis, November 2000.

[20] V. Blobel, *Linear Least Squares Fits with a Large Number of Parameters*, Universität Hamburg (1999).

[21] H1 Coll., S. Aid *et al.*, Nucl. Phys. **B545** (1999), 21.

[22] S. Hengstmann, Nucl. Phys. (Proc.Suppl.) **B79** (1999), 296.

[23] H1 Coll., C. Adloff *et al.*, Phys. Lett. **B467** (1999), 156.

[24] CDF Coll., F. Abe *et al.*, Phys. Rev. Lett. **71** (1993) 2396, Phys. Rev. **D53** (1996), 1051; D0 Coll., S. Abachi *et al.*, Phys. Rev. Lett. **74** (1995) 3548, Phys. Let. **B370** (1996), 239.

[25] M. Acciarri *et al.*, L3-Coll., preprint hep-ex/0011070; OPAL Coll., *Beauty particle production in photon-photon scattering at LEP2*, presented at ICHEP2000, Osaka, Japan, 2000.

[26] E. L. Berger *et al.*, preprint hep-ph/0012001.

[27] *The H1 Silicon Vertex Detector*, D. Pitzl *et al.*, Nucl. Instrum. Meth. **A454** (2000), 334.

[28] *Open charm and beauty production at HERA* F. Sefkow, Proc. 30^{th} Int. Conf. on High Energy Physics (ICHEP 2000), Osaka, Japan, July 2000, hep-ex 0011034.

[29] T. Sloan, talk presented for the H1-Coll. at Moriond-QCD 2001, March 2001

[30] *Measurement of Neutral and Charged Current Cross-Sections in Electron-Proton Collisions at High Q^2*, contr. # 971 in ref. [16].

[31] *Search for Compositeness, Leptoquarks and Large Extra Dimensions in e^-q and e^+q Contact Interactions at HERA*, contr. # 951 in ref. [16].

[32] *Inclusive Measurement of Deep Inelastic Scattering at high Q^2 in Positron-Proton Collisions at HERA*, contr. # 975 in ref. [16].

[33] *W production in ep collisions at HERA*, contr. # 974 in ref. [16].

[34] CTEQ-Coll., H.L. Lai *et al.*, Phys. Rev. **D55** (1997), 1280; hep-ph 9701256, hep-ph 9903282.